PLFC: The Packet Length Fuzzy Controller to Improve the Performance of WLAN under the Interference of Microwave Oven

Shiann-Tsong Sheu, Yang-Han Lee, Yao-Chun Yu, and Yu-Ching Huang, Meng-Hong Chen
Department of Electrical Engineering, TamKang University
Tamsui, Taipei Hsien, Taiwan 30043, R.O.C.
Tel: +886-2-6215656 ext 2730
Fax: +886-2-6221565
Email: stsheu@ee.tku.edu.tw

Abstract

In this paper, we have investigated the effects of microwave ovens over the IEEE 802.11 FHSS (Frequency Hopping Spread Spectrum) wireless LAN card. The measured MAC Frame Error Rate (FER) and UDP Packet Error Rate (PER) are affected by the microwave ovens. From these measurement results we know that the performance of some channels within the IEEE 802.11 FHSS wireless LAN card can be seriously deteriorated. Furthermore, decreasing the packet length would improve the transmission performance from the PER measurement results. Therefore, we design a novel fuzzy controller to dynamically adjust the packet length to against the interference from microwave oven. Simulation results show that the designed fuzzy controller can effectively improve the transmission performance in terms of throughput.

Index terms—IEEE 802.11, FHSS, Microwave Oven, Fuzzy Controller

1. Introduction

Recently, the technology of wireless communication has progressed rapidly and the wireless data communication products such as wireless LAN and wireless ATM have been investigated in laboratories. In June 1997, the IEEE 802.11 draft 6 [1] has been announced by the IEEE computer society. Many manufacturers manufacture the wireless LAN cards and some products have been brought into markets now. Because the operation frequencies of the wireless LAN card are within the ISM (Industrial, Scientific and Medical) band, there exist some extraneous sources within the same frequency band to interfere each other. Since the most significant interference in this band is caused by the microwave oven, many researches have investigated the effects by it. In paper [2], the authors have experimentally measured the interference radiated from the microwave oven and discussed the statistical characteristics of interference from the time domain. The performance improvement with Bose-Chaudhuri-Hocquenghem (BCH) code has been shown in [3]. The statistical model of microwave oven in the time domain has been shown in [4]. The interference from two kinds of microwave ovens over the wireless LAN cards has been investigated in [5]. However, few papers actually measure the interference using the wireless LAN card in terms of MAC frame error rate (FER) and UDP packet error rate (PER). Therefore, we use the IEEE 802.11 FHSS wireless LAN cards to measure the MAC FER in individual channels to obtain the interference distribution from the microwave oven. In order to demonstrate the measurement results of FER, we have measured the signal spectrum radiated by microwave oven and compared to the differences of FER. However, the FHSS system transmits data through a set of hopping sequences, we also measure the PER by transmitting the UDP frame for the sake of realistic application. According to the measurement results, we obtain that decreasing the packet length can resist effects from microwave oven. However, it is hard to precisely distinguish the interference caused by microwave oven, and determine the perfect packet length to minimize the interference. Therefore, we design a fuzzy controller with three different methods to dynamically adjust the packet length according to the interfering degree.

This paper is organized as follows. Brief introduction of IEEE 802.11 wireless LAN is given in section 2. In section 3, we describe the measurement environment and conditions. In section 4, we demonstrate the measurement results. The proposed fuzzy controller is described in section 5 and simulation model and results are shown in section 6. Finally, some conclusions of this paper are given in section 7.

2. IEEE 802.11 Wireless LAN

IEEE 802.11 draft 6 [1] has been announced in June 1997. The media access control (MAC) layer and physical (PHY) layer of wireless LAN has been defined in this standard. In order to be used in different environments, the standard defines two architectures in the MAC layer protocol which are Ad Hoc network and Infrastructure network. The benefit of Ad Hoc network (Figure 1) is that the set up time for this network is very short. However stations in the network can only communicate to each other. Therefore, if the user wants to connect to the internet, he/she must use the Infrastructure network instead of Ad Hoc network, as shown in Figure 2. In this network, stations can exchange data to the other users within the internet through an Access Point.

In the IEEE 802.11 standard, for both network architecture, there are three medium types defined in the PHY layer:

- Direct Sequence Spread Spectrum (DSSS)
- Frequency Hopping Spread Spectrum (FHSS)
- Diffused Infrared

DSSS and FHSS systems are being used in 2.4 GHz, which is the unlicensed band for ISM. Therefore, interference caused by other signal sources may affect the performance of wireless LAN card. In order to avoid the major interference, we have measured the effects from microwave oven by using the IEEE 802.11 FHSS wireless LAN cards.

3. Measurement Environment

The measurement environment and equipment are shown as Figure 3. We have used one pair notebooks connected by IEEE 802.11 FHSS wireless LAN cards to measure the effects from the operating microwave oven. The effects are measured by directly transmitting the MAC frames (UDP packets) at the transmitter and recording the frame error rate (packet error rate) at the receiver. Because channels in the FHSS system are separated by 1.0MHz from 2.4GHz to 2.5GHz in IEEE 802.11 standard, the FER is measured from channel 1 to 99 spaced by 10 channels. In order to study the relationship of the distance and directions between notebooks and microwave oven, we have designed several experimental cases as follows:

a. In order to find the effect on the receiver we consider four cases. The locations of transmitter, receiver, and microwave oven are given as Figure 4(a)-(d). We have measured the FER of the receiver from the four directions (front, back, right, and left) of microwave oven at distances from 1m to 5m. In this case, the distance between transmitter and microwave oven is 15m.

b. The locations of transmitter, receiver, cement wall, and microwave oven are shown as Figure 5. This is the general case we locate the microwave oven in the kitchen or office. In this case, we also measure the FER at different distances and the distance between transmitter and microwave oven is still 15m.

c. In order to find the microwave oven effect on the transmitter, we design the measurement environment whose the locations are indicated as Figure 6. We measure the effects to the transmitter from the microwave oven under different distances. In this case, the distance between receiver and microwave oven is 15m.

Since the FHSS system transmits data through a set of hopping sequences, we measure the PER by transmitting the UDP frames through the hopping sequences defined in the standard. In order to study the effect of PER at each direction, we measure the PER at the location as Figure 4(a)-(d). Furthermore, we also adjust the packet length from 100 to 400 bytes to study the effect of packet length to the PER.

4. Measurement Result and Discussion

In this section, we will discuss the measurement results of environments introduced in section 3. Firstly, the FER measurement results are shown as follows:

a. In Figure 7(a), the FER is under 55% in all channels for all distances. When the distance is 1m, the interference distributes from ch1 to ch50, ch70, and ch90 and the FER decreases as the distance increases. In Figure 7(b), the interference centralizes at ch40 and especially when the distance is large than 1m. In Figure 7(c)-(d), the interference distribution is almost the same and centralizes at ch40.

   From Figure 7(a)-(d), we can find that the effect is more serious in the front side of microwave oven. The effects from left and right sides are almost the same. Although the effect at the back side is critical, it's smaller than the front side. Moreover, effects are centralized around 40th channel for all directions and the interference decreased as the distance increased.

   In order to verify the results, we measure the signal spectrum radiated by microwave oven from the front, back, left, and right ends in Figure 8(a)-(d), respectively. In these figures, the central frequency is 2.450GHz and the spanning band is 200MHz. By comparing to Figures 7 and 8, the measurement results of FER are correct and the most significant interference is around ch40.

b. In Figure 9, we find that the interference would be reduced when there is a cement wall between the receiver and the microwave oven. We also find that the interference is also distributed around ch40 but the FER is under 15%.

c. From Figure 10 we obtain that the most significant interference is still around ch40. But the interference compare to case a is lower in other channels.

Table 1 lists the operating frequency range of each geographic location defined in the standard [1]. From this table we find that most channels of North America and Europe band would be interfered. However the most significant interference from microwave oven can be avoided in other geographic locations.

Figure 11 shows the measurement results about PER versus distance in four directions as the packet length is 400 bytes. From this figure we can find that the interference in the front end is most serious. However when the distance is larger than 4m, the receiver would not be interfered in the front end. Similarly, the safe distance in the back end is 2m. From these measurement results we can easily derive the safe distance in all directions when the packet length is 400 bytes.

Figure 12 shows the measurement results in the front end of microwave oven when we adjust the packet length from 100 to 400 bytes. From this figure we can see that the PER would be reduced with the decreasing of packet length. When the packet length is 100 bytes, the transmission would not be interfered no matter what the distance is. Although effects from the microwave oven can be resolved by reducing the packet length, the throughput would be degraded by the additional header overhead occupies the transmission bandwidth. Therefore, if the packet length can be adaptively adjusted, the performance would be improved under the effects of microwave oven.

In next section, we will design a fuzzy controller to dynamically adjust the packet length to maximize the network throughput.

5. The Design of Packet Length Fuzzy Controller (PLFC)

5.1 Pure Fuzzy Controller (PFC)

From previous sections we know that the adjustment of packet length will improve the throughput. However, the packet length should be dynamically adjusted because the environment situation (e.g. distance) may changes. Therefore, we design a fuzzy controller in this paper to adjust the packet length according to the environment interference.

The block diagram of the PLFC is shown in Figure 13. At first, two input linguist parameters are considered for the fuzzifier: the packet length ratio, which is denoted as *plr*, and the packet error rate, which is denoted as *per*. For input parameters, we define the corresponding fuzzy term sets: *T*(*plr*) = {Largest, Large, Small, Smallest} and *T*(*per*) = {Dangerous, Normal, Safe}. The selected membership functions for *T*(plr) and *T*(per) are the shape of Gaussian-like function (see Figures 14(a) and 14(b)). For each membership function, the peak position and the scaling factor are specified according to our knowledge about the system model. The mathematics form of the Gaussian membership function is presented as follows:

$$\mu(x) = e^{-[\frac{x-m_i}{\sigma_i}]^2}$$

where m_i and the σ_i are the peak value and the scaling factor of the *i*th membership function, respectively. We also define the term set of the output next packet length ratio *nplr* as *T*(*nplr*) = {Largest, Large, Small, Smallest}. According to the fuzzy set theory, the fuzzy rule base has $|T(plr)| \times |T(per)| = 12$ inference rules (see Table 2) which is used to decide the optimal packet length in each distance. The desired optimal packet length is calculated as follows:

$$Th(s,e) = \frac{s}{s+h} * (1-e),$$

where *s*, *e* and *h* are packet length, PER and additional header from UDP packet to the physical frame, respectively. Based on previous simulation results, we show that the PER and throughput under different distance and packet lengths in Table 3 and 4, respectively. Therefore, the optimal packet length in distances 1m, 2m, 3m, 4m and 5m are 100, 200, 200, 400, and 400 bytes, respectively. The detailed optimal packet length at each distance is shown in Figure 15.

In the inference engine, the max-min inference method [6] is used. For the *i*th rule, the corresponding membership values of these two input variables *plr* and *per* are calculated by $\mu_i(plr)$ and $\mu_i(per)$, respectively. The weight w_i used in defuzzifier is determined by the minimum value between $\mu_i(plr)$ and $\mu_i(per)$. Considering the defuzzifer in PLFC, we employ the singleton method [7] as our defuzzification strategy to reduce the complexity of computation (see

Figure 14(c)). For each fuzzy rule, the method will convert the output membership function into a crisp output control value. The singleton defuzzification method calculates the crisp output value y_l by the following equation:

$$y = \frac{\sum_{i=1}^{n} w_i \times p_i}{\sum_{i=1}^{n} w_i},$$

where $n = |T(plr)| \times |T(per)|$, p_i is the peak value of the ith output membership function of $T(nplr)$, and w_i is the weight of the ith control rule. Hence, the next packet length is $y \times Max\_Packet\_Length$, where *Max_Packet_Length* = 400bytes in this paper.

In this section, we use the fuzzy controller to dynamically adjust the packet length according to the environment interference. The target is to adjust the packet length near the optimal length shown in Figure 15. In order to close the difference, we propose two methods to improve the performance of PLFC.

5.2 Fuzzy Controller with Fine Tuning the Packet Length (FC-FTPL)

In this section, we use the fuzzy controller introduced in section 5.1 and fine tuning the packet length in each window size. As shown in Figure 16, the PFC method adjusts the packet length (*pl*) at the beginning of each transmission window and use the value *pl* as the transmission packet length in each window,

$$\begin{cases} pl_{nw}(1+lr), & \text{where } pl_{(n-1)w} > pl_{nw} \\ pl_{nw}(1-lr), & \text{where } pl_{(n-1)w} < pl_{nw} \\ pl_{(n-1)w}(1-lr), & \text{else} \end{cases}.$$

Since the adjusting length rate *lr* will effect the performance of FC-FTPL, we will discuss the value in section 6.

5.3 Fuzzy Controller with Fine Tuning the Window Size (FC-FTWS)

Although the fuzzy controller can adjust the packet length to improve the transmission performance, the length is adjusted at the beginning of each window size. If the window size is too large, the erroneous judgement would result the burst error. However, if the window is too small, the system will be unstable and change the packet length too frequently. Therefore, in this section we propose a method to dynamically tune the window size according to the transmission results.

Figure 17 is the flow chart of FC-FTWS and the value *w* is limited in range (Min_W and Max_W). As soon as the transmission packet number is large than the value Min_W, the window size *w* will be adjusted according to the PER. By this methodology, the burst error problem will be solved by dynamically decreasing the window size. On the other hand, if the PER is under the value GOOD_PER, the window size would be increased to continued transmit in the good state. In order to avoid falling into the local optimal value, we restrict the length must be adjusted when *w* = Max_W. The same as previous section, the tuning window size ratio *wr* may also effect the performance. Therefore, we will discuss it in next section.

6. The Simulation Model and Results

The simulation model is described as follows. We simulate the notebook initially located at 3 meter away from the microwave oven and moving around at the front end of the microwave oven. The moving range in this paper is between 1m and *R*m. The total simulation time is *T* time units and at each time unit, the notebook would decide to move or not according to the moving probability *mp*. Once it decides to move, the moving rate *mr* is used to derive the distance between it and microwave oven, and the moving direction is equal in forward or backward. Besides, the notebook would transmit UDP packets to the receiver and the number is an exponential distribution with a mean of *L* packets. The notebook would use the PLFC to adjust the packet length according to *plr* and *per* in order to get better transmission performance. The packet error rate *per* is calculated after transmitting *w* packets and the parameter *w* is the window size. In order to evaluate the performance of PLFC and normal fixed length methods, we use the following metrics:

Transmission Data Rate (TR) = the ratio of the total payload (without considering the header) which are successfully received and the simulation time *T*.

Transmission Efficiency (TE) = $\frac{d_S}{(d_S + h_S) + (d_F + h_F)}$, where d_S and h_S are the amount of payload and header which was received successfully, respectively, and d_F and h_F are the amount of payload and header which was received failed, respectively.

Average Differential Value (ADV) = the average differential value of the transmission packet length and optimal packet length of its location which packets are transmitted.

Successful Rate (SR) = the ratio of the number of packet which was received successfully to the number of packet being transmitted.

Following, we show the simulation results. In this simulation, the simulation time *T* is 1,000,000 time units and the parameter *L, R* are equal to 5 and 6, respectively.

Firstly, we shows the results of PFC method introduced in section 5.1. From Figures 18 to 21, we show the TR, TE, ADV, and SR versus the moving probability *mp* as *w* = 5, 10, 15, and 20. From these results we can find that when *w* is small, the SR is lower than other values. This result leads the TR and TE are lower than other values and the average differential value of ADV are large. This is because that the system will become unstable when window size is small. Therefore, we design another two methods FC-FTPL and FC-FTWS to improve the performance of the system.

Furthermore, the moving rate may also effect the simulation results. Therefore, we compare the results when the *mr* = 0.3, 0.6, and 0.9. In Figure 22 we can find that the performance of PFC is more stable when the moving rate *mr* = 0.6 and 0.9 than *mr* = 0.3. This is because that when the *mr* is small, the station may continued stay at the same location. This leads to that the performance will be effected seriously by the location especially when the simulation time is not long enough. Therefore, we compare the PFC method and normal fixed length method when *mr* = 0.6.

From previous results we can find that *w* = 5 and 20 are the worst and best results. Therefore, we using these results compare to the normal fixed length method. Figure 23 is the TR with and without PFC. From these results we can find that the performance of PFC is better than normal fixed length method no matter what window size is. Because using the PFC will transmit the short packet in order to avoid the interference, this will lower the transmission efficiency. Therefore, in Figure 24, the TTE is lower than length=200 when *w* = 5. However, the results are always better than normal fixed length method as *w* = 20.

From Figures 25 to 27, we show the TR, ADV, and SR using FC-FTPL under different *lr*. From these figures we can find that the better value of *lr* is about 0.05. Although the SR is better when *lr* is less than 0.05, the difference is very small.

From Figure 28 to 30, we show the TR, ADV, and SR using FC-FTWS under different *wr* and the simulation parameters BAD_PER, GOOD_PER, Max_W, and Min_W are equal to 0.3, 0.1, 10, and 5, respectively. Among these figures we can obtain that the performance is better as *wr* = 0.4 than other values. Although the SR is not the best as *wr* = 0.4, the difference is small. Finally, we compare these three methods PFC, FC-FTPL, and FC-FTWS from

Figure 31 to 33. Among these figures, we use the best parameters in each method which indicate that the *lr* is equal to 0.05 in FC-FTPL and *wr* = 0.4 is in FC-FTWS. We can find that the best result about TR is FC-FTPL, however FC-FTWS can obtain the lowest differential value of ATDV and highest SR.

7. Conclusion

From these experimental measurement results of FER, we find that the effects from microwave oven to the transceiver are serious in some channels. Furthermore, from the measurement results of PER we find that the safe distance is 4m from the microwave oven and the PER would be reduced by decreasing the packet length. However the bandwidth would be wasted on additional header. Therefore, we must care about the location of microwave oven when using the wireless LAN in office or residence. In order to resist the interference from microwave oven, we design three packet length fuzzy controllers in this paper. The simulation results show the performance is better than the normal fixed length method. The PLFC may also be used in the other situations when the transmission environment is too noisy or in other applications.

REFERENCES

[1] Part 11: Wireless LAN Medium Access Control (MAC) and Physical Layer (PHY) Specifications , the IEEE standards.

[2] Shinichi Miyamoto and Norihiko Morinaga, "Effect of microwave oven interference on the performance of digital radio communications systems", ICC '97, vol.1, pp.51 - 55

[3] Shinichi Miyamoto and Norihiko Morinaga, "Performance of digital radio communication system with BCH coding under microwave oven interference", Electronics Letters, Vol. 34, 23 July 1998, pp.1465 – 1466

[4] Hideki Kanemoto, Shinichi Miyamoto, and Norihiko Morinaga, "Statistical model of microwave oven interference and optimum reception", ICC 98, vol.3, pp.1660 - 1664.

[5] Ad Kamerman and Nedim Erkocevic, "Microwave oven interference on wireless LANs operating in the 2.4 GHz ISM band", PIMRC '97, vol.3, pp.1221 – 1227.

[6] H. J. Zimmermann, "Fuzzy Set Theory and its Application", 2nd, revised edition, Kluwer Academic Publishers, pp. 11-17, 1991.

[7] R.R. Yager, L.A. Zadeh, "An Introduction to Fuzzy Logic Application in Intelligent System," Kluwer Academic Publishers, 1992.

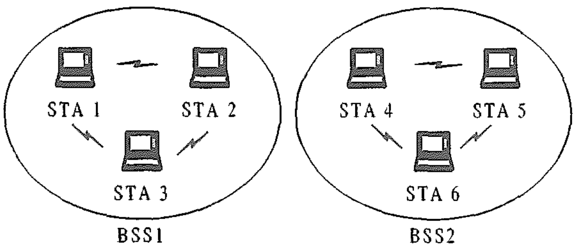

Figure 1. Ad Hoc Network

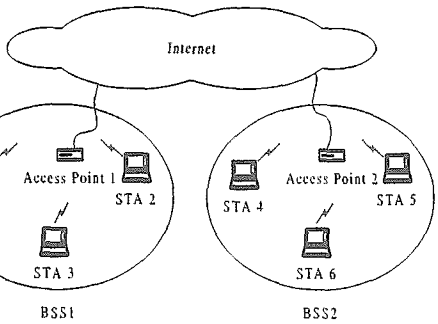

Figure 2. Infrastructure Network

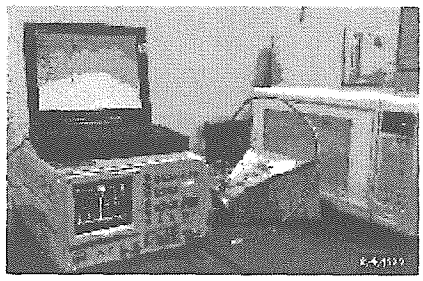

Figure 3. Experimental environment and equipment

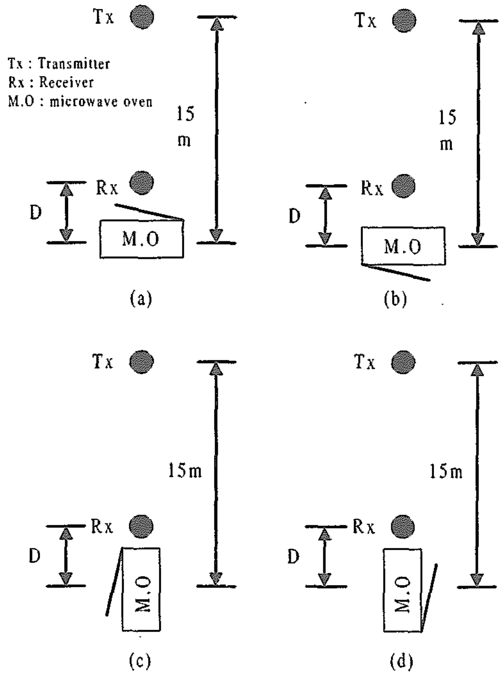

Figure 4. Measurement environment in case a

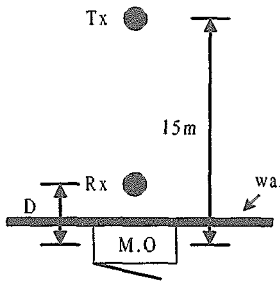

Figure 5. Measurement environment in case b

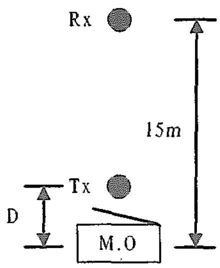

Figure 6. Measurement environment in case c

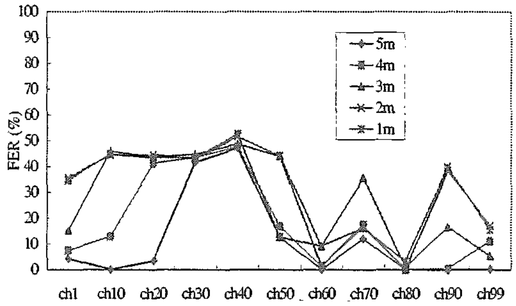

(a). The front side

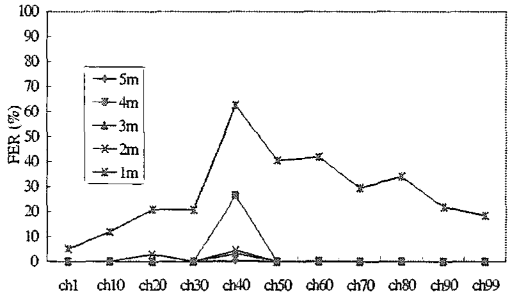

(b). The back side

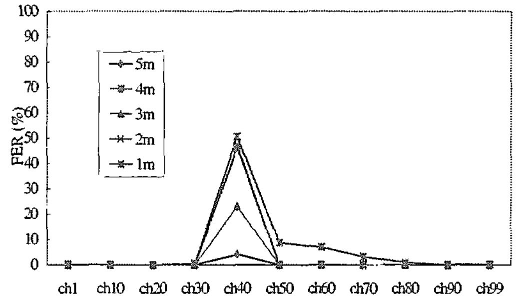

(c). The left side

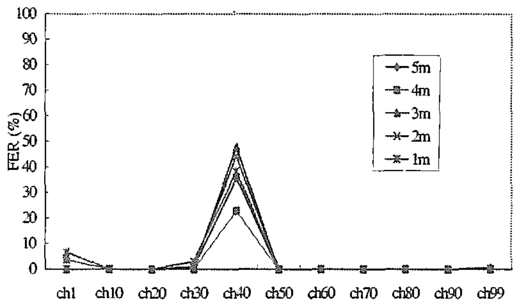

(d). The right side

Figure 7. The measurement results in different sides

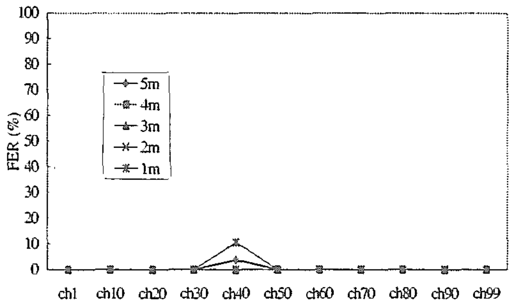

Figure 8. The measurement results obstructed by the cement wall

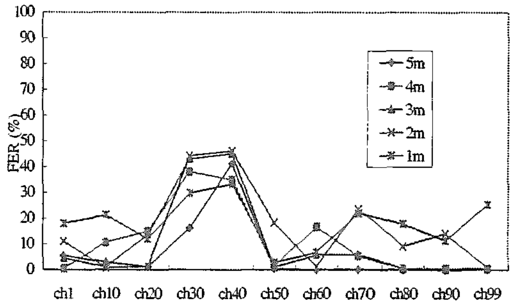

Figure 9. The measurement results in case c

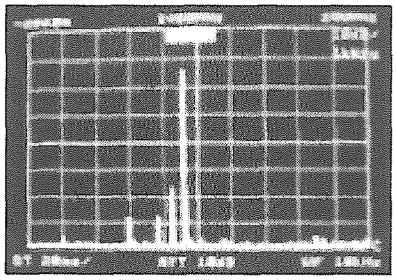

(a). In the front end

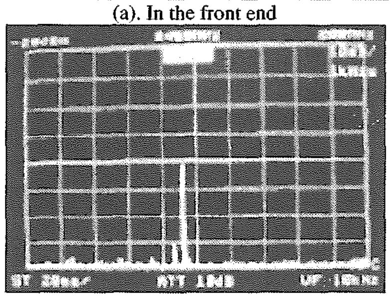

(b). In the back end

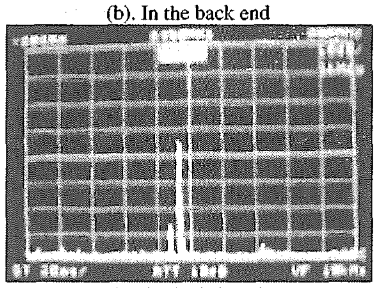

(c). In the left end

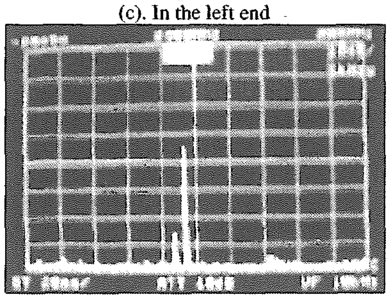

(d). In the right end

Figure 10. The spectrum measured in different ends

Table 1. The operating frequency range in each geographic location

Lower limit (GHz)	Upper limit (GHz)	Regulatory range (GHz)	Regulatory Channels	Geography
2.402	2.480	2.400~2.4835	Ch2~Ch80	North America
2.402	2.480	2.400~2.4835		Europe*
2.473	2.495	2.471~2.497	Ch73~Ch95	Japan
2.447	2.473	2.445~2.475	Ch47~Ch73	Spain
2.448	2.482	2.4465~2.4835	Ch48~Ch82	France
*Excluding Spain and France				

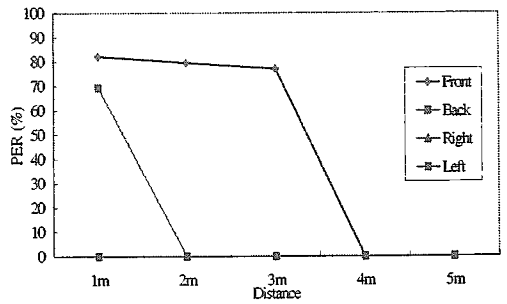

Figure 11. The measurement results of PER in four directions

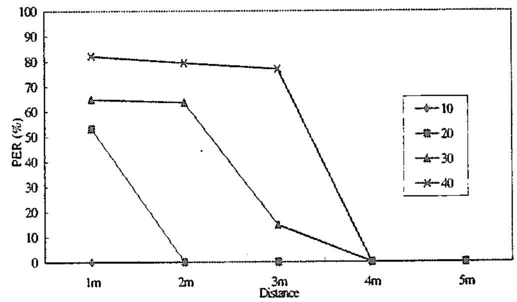

Figure 12. The measurement results of PER in different packet length

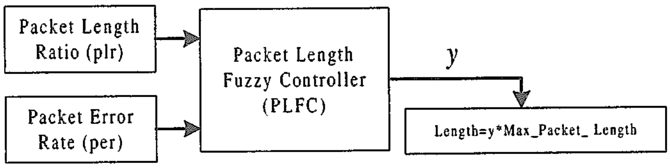

Figure 13. The block diagram of PLFC

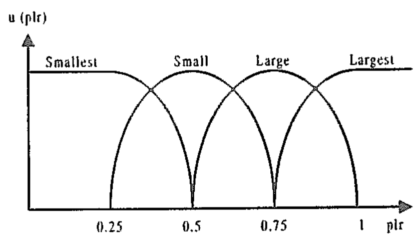

(a) T(plr)

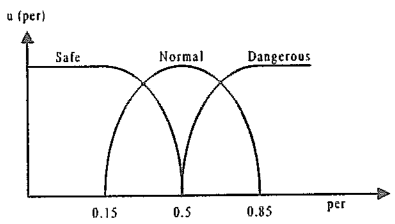

(b) T(per)

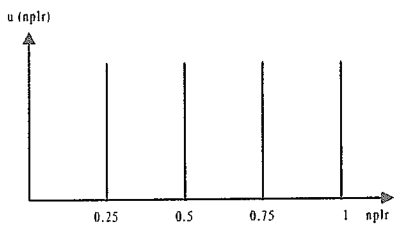

(c) T(nplr)

Figure 14. The membership functions of the term sets

Table 2. The fuzzy rules for next packet length ratio.

Rule	plr	per	nplr
1	Largest	Dangerous	Small
2	Large	Normal	Large
3	Small	Safe	Largest
4	Smallest	Dangerous	Smallest
5	Largest	Normal	Small
6	Large	Safe	Largest
7	Small	Dangerous	Smallest
8	Smallest	Normal	Large
9	Largest	Safe	Largest
10	Large	Dangerous	Small
11	Small	Normal	Small
12	Smallest	Safe	Smallest

Table 3. The PER in different distance and packet size.

PER	1 m	2m	3m	4m	5m
100	0	0	0	0	0
200	0.5331	0	0	0	0
300	0.6491	0.6372	0.1478	0	0
400	0.8214	0.7945	0.7698	0	0

Table 4. The calculation of optimal packet length under different distances.

Throughput	1 m	2m	3m	4m	5m
100	**0.5457**	0.5457	0.5457	0.5457	0.5457
200	0.3262	**0.6987**	**0.6987**	0.6987	0.6987
300	0.2703	0.2794	0.6564	0.7702	0.7702
400	0.1451	0.1669	0.1870	**0.8122**	**0.8122**
Optimal size	100	200	200	400	400

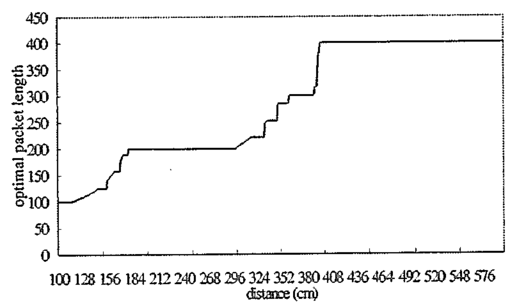

Figure 15. The optimal length in each distance

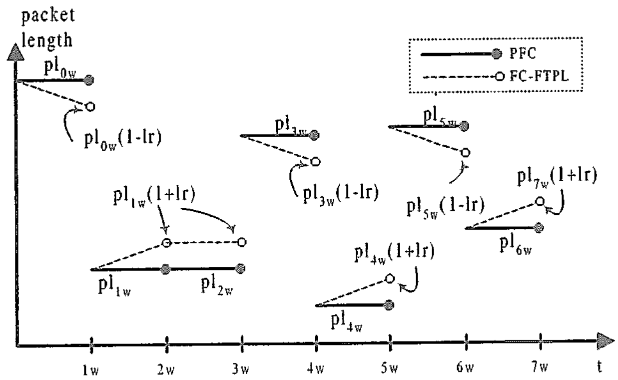

Figure 16. The packet length adjusted function of PFC and FC-FTPL

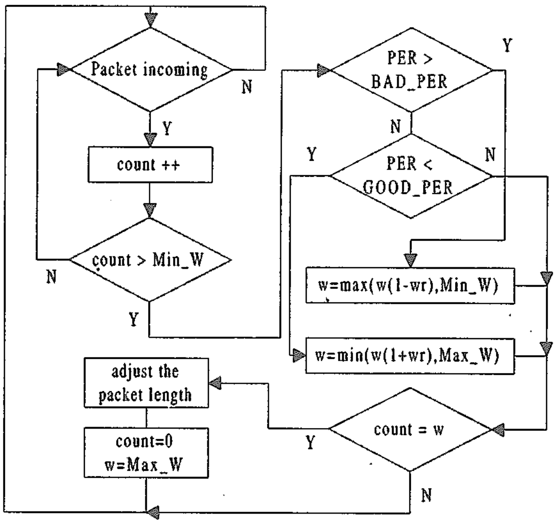

Figure 17. The flow chart of FC-FTWS

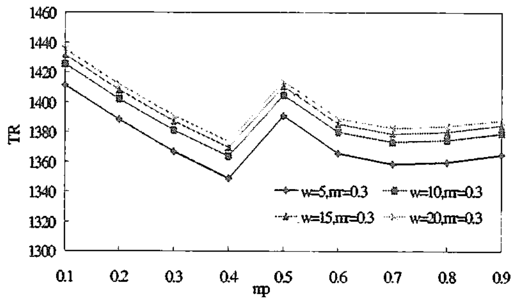

Figure 18. The TR under different window size when mr=0.3

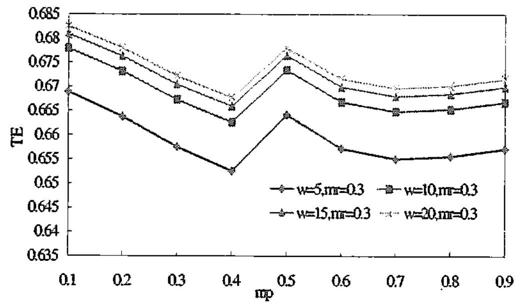

Figure 19. The TE under different window size when mr=0.3

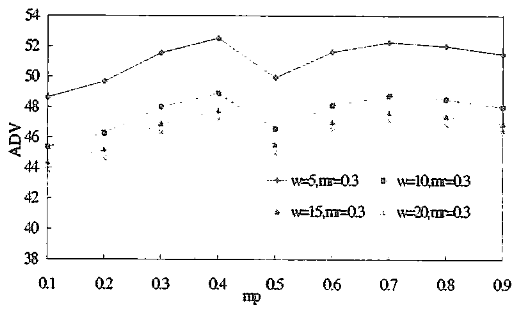

Figure 20. The ADV under different window size when mr=0.3

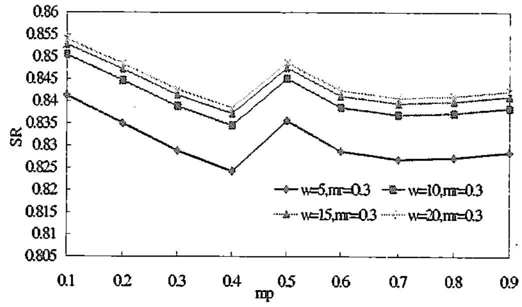

Figure 21. The SR under different window size when mr=0.3

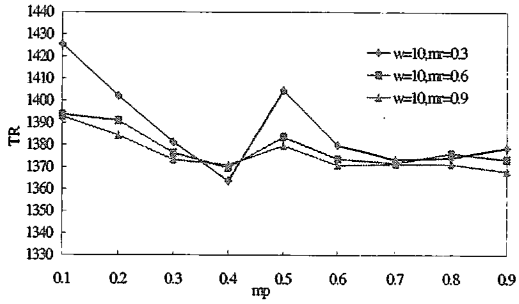

Figure 22. The TR under different mr when w=10

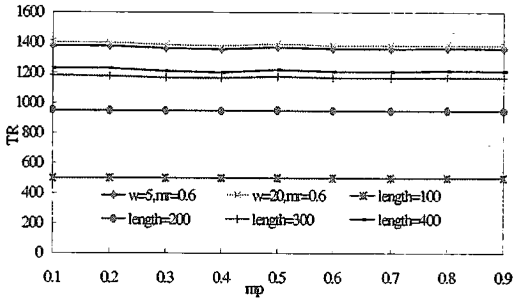

Figure 23. The comparison of TR with and without PFC

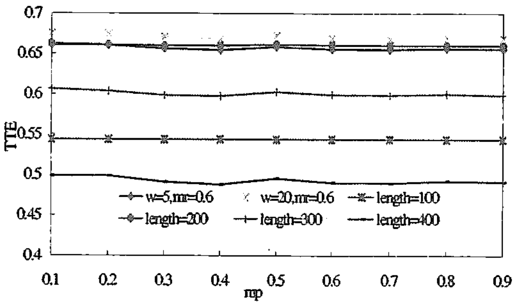

Figure 24. The comparison of TTE with and without PFC

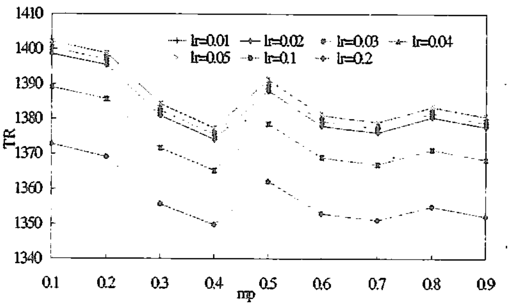

Figure 25. The TR under different lr using FC-FTPL

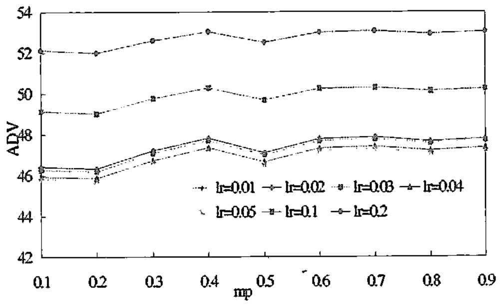

Figure 26. The ADV under different lr using FC-FTPL

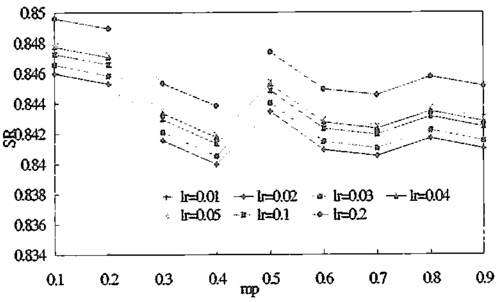

Figure 27. The SR under different lr using FC-FTPL

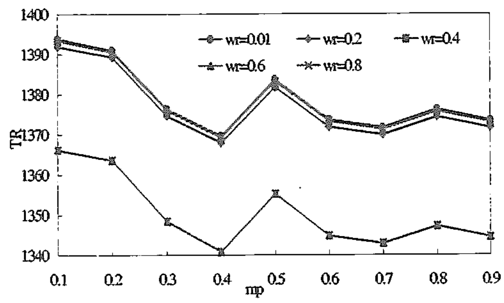

Figure 28. The TR under different wr using FC-FTWS

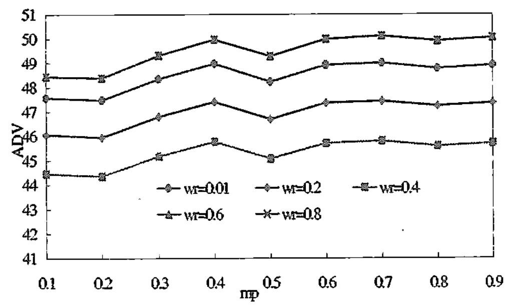

Figure 29. The ADV under different wr using FC-FTWS

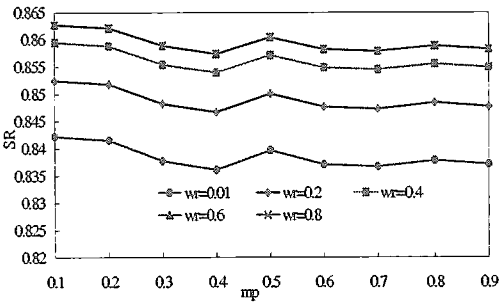

Figure 30. The SR under different wr using FC-FTWS

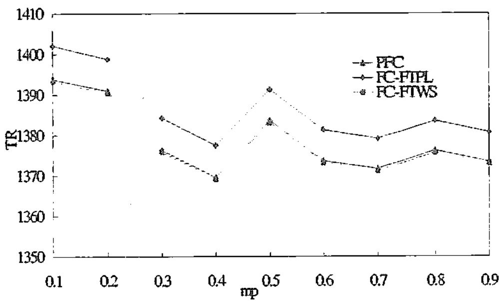

Figure 31. The comparison of TR using PFC, FC-FTPL, and FC-FTWS

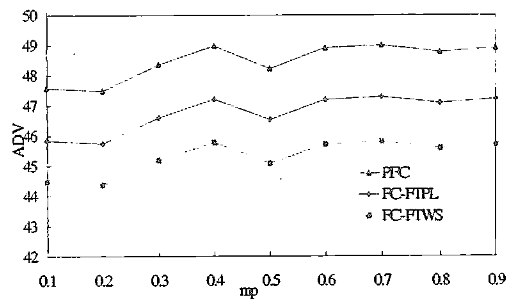

Figure 32. The comparison of ADV using PFC, FC-FTPL, and FC-FTWS

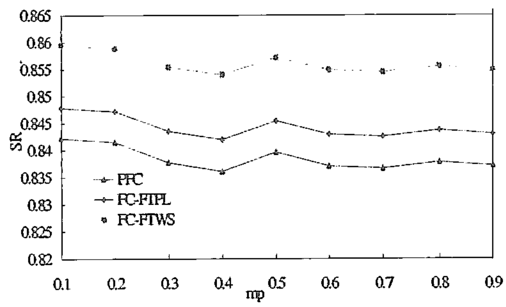

Figure 33. The comparison of SR using PFC, FC-FTPL, and FC-FTWS